

# Joint shear strength prediction for reinforced concrete beam-to-column connections

Mehmet Unal\* and Burcu Burak<sup>a</sup>

*Department of Civil Engineering, Middle East Technical University, Ankara, Turkey*

*(Received December 2, 2010, Revised September 29, 2011, Accepted January 13, 2012)*

**Abstract.** In this analytical study numerous prior experimental studies on reinforced concrete beam-to-column connections subjected to cyclic loading are investigated and a database of geometric properties, material strengths, configuration details and test results of subassemblies is established. Considering previous experimental research and employing statistical correlation method, parameters affecting joint shear capacity are determined. Afterwards, an equation to predict the joint shear strength is formed based on the most influential parameters. The developed equation includes parameters that take into account the effect of eccentricity, column axial load, wide beams and transverse beams on the seismic behavior of the beam-to-column connections, besides the key parameters such as concrete compressive strength, reinforcement yield strength, effective joint width and joint transverse reinforcement ratio.

**Keywords:** reinforced concrete; beam-to-column connections; joint shear strength; cyclic loading

---

## 1. Introduction

Beam-to-column connections experience considerable deformations under earthquake loading and therefore, play an important role in the seismic behavior of reinforced concrete structures. If these regions are not properly designed and detailed, they fail prematurely under strong earthquake ground motions. In order to understand the behavior of beam-to-column connections in more detail, numerous experimental and analytical studies have been carried out for more than 40 years. Many researchers investigated the parameters influencing joint behavior and some came up with joint models that predicts the connection behavior under earthquake loading.

Durrani and Wight (1985) investigated interior beam-to-column connections under earthquake loading and concluded that joint shear stress has a significant influence on seismic performance of connections. In other words, strength degradation, stiffness loss, crack development and drift are affected by the level of joint shear stress. Therefore, shear reinforcement ratio which is parallel to the plane of loading is one of the most important parameters for maintaining a desired ductility level. Ehsani and Wight (1985) conducted an experimental study on the behavior of exterior reinforced concrete beam-to-column connections subjected to earthquake loading. Six specimens

---

\*Corresponding author, Ph.D. Candidate, E-mail: [umehmetu@gmail.com](mailto:umehmetu@gmail.com)

<sup>a</sup>Assistant Professor

were tested and the effects of different parameters influencing connection behavior are investigated. In this study, parameters such as the moment strength ratio, joint transverse reinforcement ratio and joint shear stress levels given by the code requirements were found to be conservative.

There are also numerous experimental studies focusing on the effect of a specific parameter. Raffaele and Wight (1995) examined the effect of eccentricity on the performance of beam-to-column connections and observed that eccentric beam-to-column connections have a reduced joint strength. Chen and Chen (1999) tested six beam-to-column connection specimens five of which were eccentric and concluded that the subassemblies with eccentricity between the column and beam centerlines had lower stiffness and energy dissipation capacities. Teng and Zhou (2008) also stated that joint eccentricity slightly reduces the story shear strength and lateral stiffness of the connections. Burak (2005), Burak and Wight (2008) investigated the effect of the floor system on the behavior of eccentric connections and observed that if the transverse beams and the slab is included in the test set up, the strength reduction due to eccentricity significantly decreases. Shin and LaFave (2004) also investigated eccentric connections with floor slabs and found out that floor slabs increased the joint shear strength and diminished differences between the seismic performance of eccentric and concentric connections.

Material properties are influential on the joint shear capacity. Ehsani and Alameddine (1991) carried out experiments on high-strength reinforced concrete connections and realized that high concrete compressive strength results in high shear capacity but decreases ductility. Kaku and Asakusa (1991) examined the ductility of exterior beam-column subassemblies when diverse amount of axial load, between 0 - 17% axial load capacity of the column, was applied. It was observed that joint shear strength was higher when higher axial loads were applied to the column. When Fujii and Morita (1991) compared the joint behavior of interior and exterior reinforced concrete connections, it was monitored that exterior joints had 10% to 20% less shear strength than interior joint subassemblies.

Presence of wide beams also affects the behavior of beam-to-column connections. LaFave and Wight (1999) tested three exterior wide beam-column-slab subassemblies under quasistatic cyclic loading and concluded that wide beams influenced the joint behavior positively by providing extra confinement. Quintero-Febres and Wight (2001) tested three interior wide beam-column-slab connections under cyclic loading. The experimental results show that wide beam interior connections can withstand large drifts without significant strength and stiffness degradation. However, Burak and Wight (2008) observed that if the depth of the wide beam is not sufficient to provide the necessary confinement to the connection region, the joint shear strength reduces and the joint shear distortions significantly increase.

Based on the experimental results, numerous analytical studies have been conducted to investigate the effect of different parameters on joint shear strength and propose analytical models to represent the seismic behavior of the connection region. Lowes and Altoontash (2003) developed a joint model that is composed of a four node 12 degree of freedom element connecting beam and column elements which takes into account parameters on detailing, geometry and material properties. Shin and LaFave (2004) investigated the effects of some key parameters such as concrete compressive strength, joint reinforcement and axial load effect on the joint shear strength. An analytical method was proposed in this study to estimate the hysteretic joint shear stress versus strain behavior by employing modified compression field theory. Mitra and Lowes (2007) utilized a numerical simulation of the parameters in conjunction with finite element analysis to predict the joint shear strength. More recently, Kim and LaFave (2008) used statistical methods to evaluate the effect of

concrete compressive strength, panel geometry, confinement due to joint reinforcement, column axial compression and bond demand level of the longitudinal reinforcement on the joint behavior. It was concluded that joint shear capacity mostly depends on concrete compressive strength; however, joint panel geometry has only a slight effect on seismic performance.

Based on the findings of previous experimental and analytical studies, key parameters that influence the joint shear strength were selected and a database was constructed to investigate the effect of these parameters on the seismic behavior of beam-to-column connections. The joint shear strength is estimated statistically by using Bayesian parameter estimation approach. The comparison of the shear strength prediction with the experimental data and the improvement over the current code requirements are presented in this paper.

## 2. Database collection

A database of experimental results is generated in order to be used in the prediction of the joint shear strength of reinforced concrete beam-to-column connections. Experimental studies involving both interior and exterior connections tested under cyclic loading are investigated. Experiments that contain data on joint shear response including joint shear strength and distortions were selected for the database to ensure adequate levels of shear deformations in the specimens that are included in the joint shear strength prediction. The database also contains subassemblies with wide beams, slabs and/or transverse beams. Moreover, in order to investigate the effect of eccentricity on the joint shear strength, specimens that have eccentricity between the centerlines of the longitudinal beams and the column are also included in the database. All connection subassemblies in this database have strong column-weak beam behavior. The experimental database consists of 92 specimens from 17 different research projects. Table 1 summarizes the type of specimens that are considered in this

Table 1 Connection types in the database

	Interior	Exterior	TOTAL:
Connections having Code Compliant Joint Transverse Reinforcement	16	31	47
Connections not having Code Compliant Joint Transverse Reinforcement	20	25	45
Connections with Applied Axial Load	25	43	68
Connections without Applied Axial Load	11	13	24
Connections with Square Columns	24	47	71
Connections with Rectangular Columns	12	9	21
Connections with Conventional Beam	33	48	81
Connections with Wide Beam	3	8	11
Connections with Slab	16	6	22
Connections without Slab	20	50	70
Connections with Eccentricity	13	4	17
Connections without Eccentricity	23	52	75
TOTAL:	36	56	92

analytical study in terms of number of interior and exterior specimens and the number of specimens having code compliant joint transverse reinforcement (ACI-ASCE Committee 352 2002), applied axial load, rectangular columns, wide beams, slabs and eccentricity.

Prior studies indicated that the effective joint width is an important parameter for the seismic behavior of the connection region. Thus, effective joint width is calculated for all specimens following the guidelines of ACI-ASCE Committee 352 Recommendations (2002). Moreover, the effective joint width recommended by LaFave *et al.* (2005) was also considered in the predictions while developing the proposed formula. For wide beams, effective joint width recommended by Burak (2005), Burak and Wight (2008) was used in the computations. These effective joint width definitions are presented below

1) ACI-352 Recommendations (2002) define the effective joint width as the smallest of

$$b_j = \frac{b_b + b_c}{2}; \quad b_j = b_b + \sum \frac{m \cdot h_c}{2}; \quad b_c \quad (1)$$

2) LaFave *et al.* (2005) define the effective joint width as

$$b_j = \frac{b_b + b_c}{2} \quad (2)$$

3) Burak and Wight (2008) define the effective joint width of connections with wide beams as

$$b_j = b_c + \frac{1}{4} \cdot (b_b - b_c) \quad (3)$$

where,  $b_b$  is the width of the longitudinal beam,

$b_c$  is the column width perpendicular to the direction of loading,

$h_c$  is the full depth of column,

$m$  is the slope to define effective width of joint transverse to the direction of shear. For joints where the eccentricity between the beam centerline and the column centroid exceeds  $b_c/8$ ,

$m = 0.3$ ; for all other cases,  $m = 0.5$ .

The procedure for determining  $m$  and the effective joint width when the beam width is less than the column width is illustrated in Fig. 1.

In the database,  $v_{j,max}$  is obtained by dividing maximum joint shear force observed in the test to the effective joint area, which is the multiplication of effective joint width and column depth. When the experimental results did not include maximum shear forces or stresses, strain gage data for top

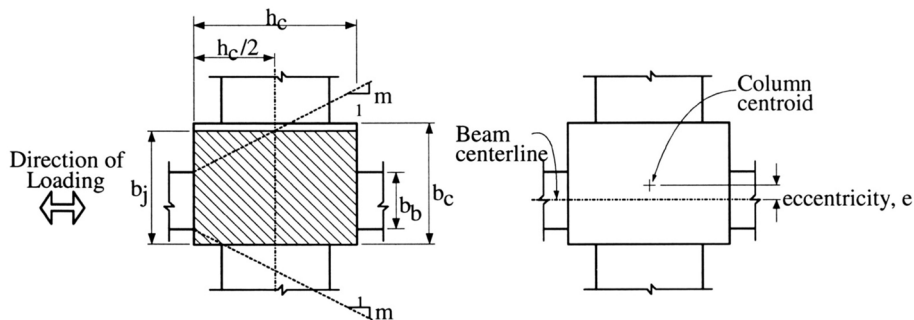


Fig. 1 Effective joint width (ACI-ASCE Committee 352-02 (2002))

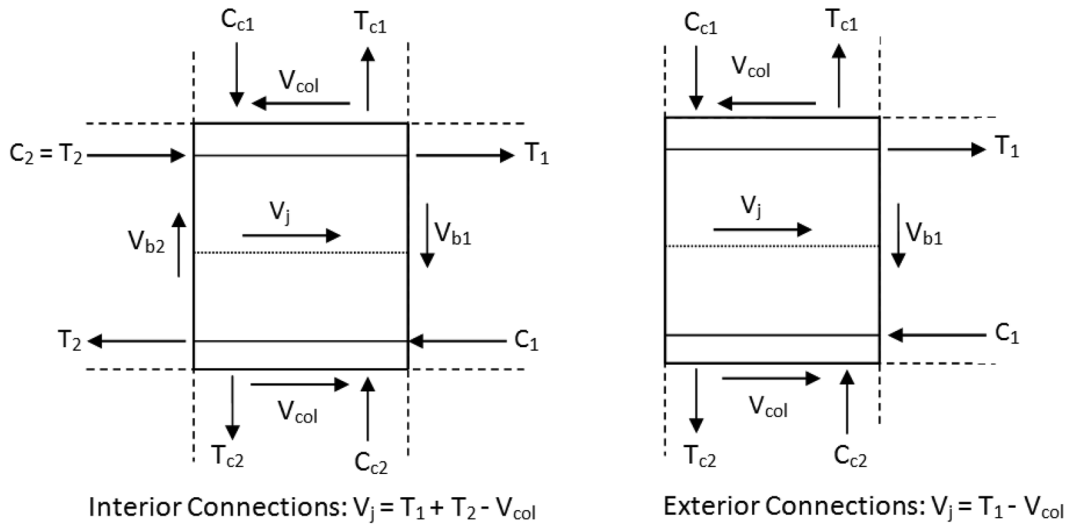


Fig. 2 Computation of joint shear in exterior and interior connections (2002)

and bottom longitudinal beam reinforcement was utilized to calculate joint shear force. By using tensile forces on the longitudinal bars, joint shear stresses were computed as shown in Fig. 2. In this figure, tensile forces ( $T_1$  and  $T_2$ ) are calculated using Eq. (4), where the stress multiplier of 1.25 accounts for having a higher than nominal yield strength and strain hardening of reinforcing bars as in ACI 352R-02 (2002). In this figure,  $C$  denotes compression force and  $V$  denotes shear force. Subscripts  $c$  and  $b$  stand for column and beam, respectively and  $V_{col}$  is the horizontal column shear force.

$$T = (1.25) \cdot A_s \cdot f_y \quad \text{if} \quad \varepsilon_s \geq \varepsilon_y$$

$$T = A_s \cdot \varepsilon_s \cdot E_s \quad \text{if} \quad \varepsilon_s < \varepsilon_y \quad (4)$$

where,  $A_s$  is the area,  $f_y$  is the yield strength,  $\varepsilon_s$  is the strain and  $E_s$  is the modulus of elasticity of the reinforcing bars.

### 3. Parameters affecting the joint behavior

Prior experimental studies indicated that material strength of both concrete and steel play an important role in joint shear capacity. Moreover, confinement is an important factor affecting the joint behavior. Confinement is either provided by the transverse reinforcement in the joint or by the transverse beams and slab framing into the connection region. Joint core should be properly confined in order to transfer shear forces, anchor beam reinforcement and transmit the column axial load. Volumetric confinement ratio is determined by computing the volume of transverse reinforcement in the connection region and dividing it by either core or gross volume or the effective volume for one layer of transverse reinforcement. The ratio which gives the best

Table 2 Correlation of key parameters with experimental joint shear strength

$v_{j,max}$ ( $b_j$ , Eq. 3&4)	$f_c$	$f_y$	$\rho_{core}$	$\rho_{gross}$	$\rho_{onelayer}$	$b_c$	$h_c$	$b_b$	$h_b$	$N$	$e$
Exterior	0.6598	-0.0637	0.4559	0.3299	0.5197	-0.2987	-0.4156	-0.4151	0.1781	0.3726	-0.2299
Interior	0.6858	0.1002	0.2473	0.2821	0.5542	0.0275	0.1285	-0.1734	0.0101	0.2159	-0.4258
$v_{j,max}$ ( $b_j$ ,352)	$f_c$	$f_y$	$\rho_{core}$	$\rho_{gross}$	$\rho_{onelayer}$	$b_c$	$h_c$	$b_b$	$h_b$	$N$	$e$
Exterior	0.6693	0.0790	0.4512	0.3101	0.5356	-0.1393	-0.3189	-0.2319	0.2963	0.3292	-0.2471
Interior	0.6929	0.0850	0.3608	0.3546	0.5604	0.0996	0.1996	-0.1032	0.0353	0.1564	-0.3349

correlation with the experimental results is taken as a contributing factor for the determination of the joint strength. Furthermore, axial load acting on the column, column and beam dimensions and eccentricity between the column and longitudinal beam centerlines are other factors affecting the joint shear strength.

In order to evaluate the influence of different parameters on joint shear strength, a correlation coefficient defined in Eq. (5) is considered. In this statistical approach,  $y$  is taken as joint shear strength and  $x$  is taken as the independent variable. The variables and their linear correlations with joint shear strength are presented in Table 2. Although these correlation values are rough estimates for the effect of parameters on the shear strength since the relationships are expected to be nonlinear, a simple comparative relationship between the shear strength and each variable is obtained. Although the individual parameters can be correlated with each other, the cross-correlation is not taken into account since the aim at this step is to get an idea on how much the parameters are related to joint shear strength. As it can be concluded from Table 2, concrete compressive strength has the highest correlation with the joint shear capacity. Moreover, reinforcement ratio and axial load has high correlation coefficients whereas joint geometry has only a slight effect.

$$\text{Correlation}(x,y) = \frac{\sum(x-\bar{x}) \cdot (y-\bar{y})}{\sqrt{\sum(x-\bar{x})^2 \cdot \sum(y-\bar{y})^2}} \quad (5)$$

#### 4. Joint shear strength prediction

After the correlation coefficients are obtained, the key parameters that need to be considered in joint strength prediction are selected. As mentioned before, the most influential parameters are concrete compressive strength and volumetric joint reinforcement ratio, which indicates the confinement provided by the transverse reinforcement. Therefore, stirrup area, spacing, number of layers of transverse reinforcement, joint core and gross area values are obtained. Volumetric transverse reinforcement ratio is computed in three different ways considering the effective confined volume as the gross connection volume, joint core volume and the effective volume that contains one layer of joint transverse reinforcement as given in the following equations respectively

$$\rho_{gross} = \frac{n \cdot A_o \cdot l_{eff}}{h_c \cdot b_c \cdot h_b}, \quad \rho_{core} = \frac{n \cdot A_o \cdot l_{eff}}{h_{c,core} \cdot b_{c,core} \cdot h_{b,core}}; \quad \rho_{onelayer} = \frac{A_o \cdot l_{eff}}{h_{c,core} \cdot b_{c,core} \cdot s} \quad (6)$$

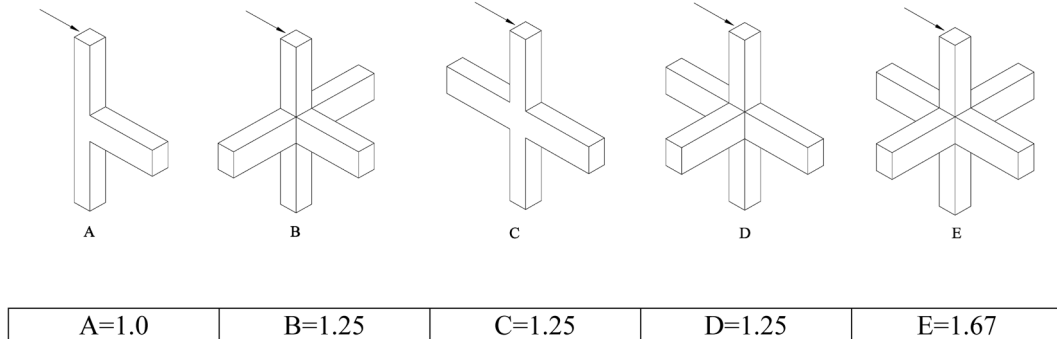


Fig. 3 Joint types and joint type index (*JT*) values for computations in SI units

where,  $n$  is the number of layers of transverse reinforcement in the effective confined area,  $A_o$  is the cross-sectional area of the transverse reinforcement,  $l_{eff}$  denotes the total effective length of the lateral reinforcement in the loading direction, which is taken as the summation of the lengths of stirrup legs placed parallel to the loading direction,  $b_c$  is the column width,  $h_c$  and  $h_b$  represent the depth of the column and beam respectively,  $s$  is the spacing of the transverse reinforcement and core is the volume of the connection region in between the longitudinal beam and column bars. Table 2 indicates that  $\rho_{onelayer}$  has higher correlation value when compared to  $\rho_{core}$  and  $\rho_{gross}$ , therefore,  $\rho_{onelayer}$  is used in the formula. On the other hand, when joint geometry is considered, it is observed that full depth of the column has the highest correlation coefficient. Furthermore, it is determined that axial load and eccentricity effects should be included in the proposed formula. In order to make an accurate prediction for the joint shear strength, first, effect of the joint type (interior or exterior) and number of transverse beams confining the connection region were taken into consideration. In the resulting formula, contributing parameters are selected as concrete compressive strength ( $f_c$ ) in the joint, joint transverse reinforcement yield strength ( $f_y$ ), joint volumetric ratio for one layer of transverse reinforcement ( $\rho_{onelayer}$ ), effective joint width ( $b_j$ ), column depth ( $h_c$ ), eccentricity ( $e$ ), and axial load ( $N$ ). Based on these individual parameters, some key parameters are defined to develop the joint shear prediction equation, which are described in detail in the thesis by Unal (2010), but are also briefly explained here.

Interior and exterior connections behave differently under seismic loading due to the confinement of the joint by the transverse beams. In order to take this into account, a parameter, defined as *JT* (Joint Type Index), is included in the equation. For different joint types, ACI-ASCE Committee 352 recommendations (2002) are followed while determining the values of the joint type indices. Connection subassemblies investigated in this study are divided into five categories from A to E, and joint types and corresponding joint type index values are given in Fig. 3.

The joint type index was then multiplied with both concrete compressive strength and transverse reinforcement yield strength in the connection region. In order to have a close prediction of the shear strength, different powers of  $f_c$  and  $f_y$  were evaluated. Eventually, the closest prediction was obtained for the power “1/6” for both  $f_c$  and  $f_y$ . The predicted shear strength at the end of this step was  $JT \cdot (f_c \cdot f_y)^{1/6}$ . After this step, the prediction was enhanced by including the effects of other key parameters. The influence of these individual parameters on the predicted strength are presented in Fig. 4.

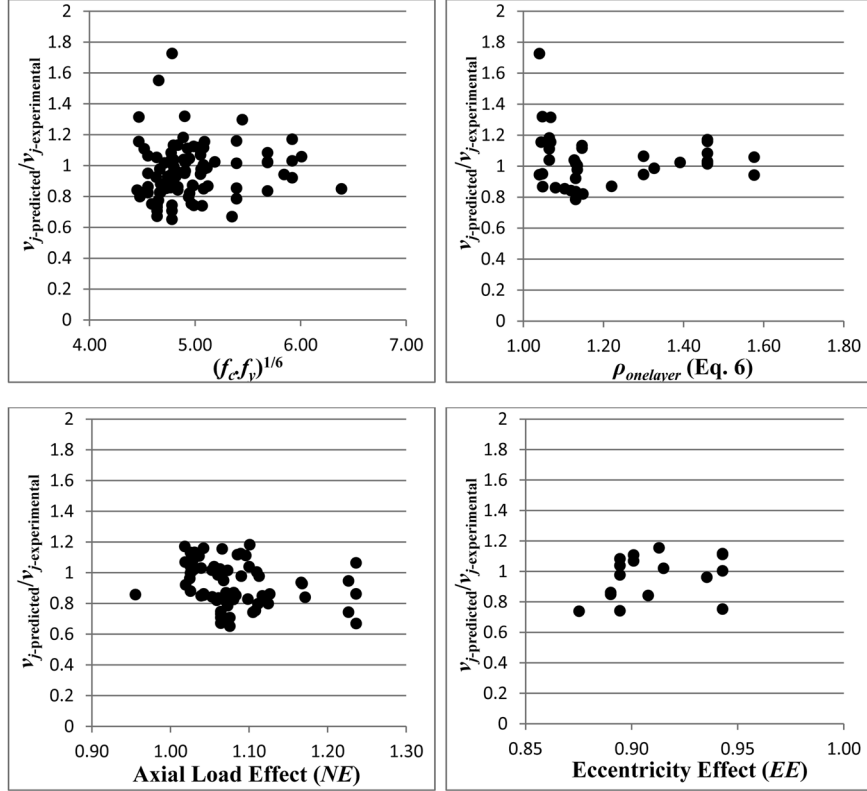


Fig. 4 Influence of individual parameters on the predicted strength

As stated before, one of the most effective parameters on joint shear strength is the volumetric reinforcement ratio for one layer of transverse joint reinforcement. Thus, all the variables are multiplied with  $\rho_{\text{onelayer}}$  and a better prediction is obtained. From the database, it is observed that when  $\rho_{\text{onelayer}}$  is less than 1.0, its effect on the shear strength is negligible, which indicates even if the confinement level is fairly low, the joint shear strength should not be reduced lower than a limiting value. Moreover, it is seen that there is not a linearly proportional relationship between volumetric joint reinforcement ratio and shear strength. Therefore, the square root of  $\rho_{\text{onelayer}}$  is used when  $\rho_{\text{onelayer}}$  is greater than 1.0. As a result, the following equation is used to define the effect of volumetric joint reinforcement ratio, which is called  $\rho_{\text{joint}}$

$$\begin{aligned} \rho_{\text{joint}}(\%) &= 1.0 & \text{if } \rho_{\text{onelayer}} < 1.0 \\ \rho_{\text{joint}}(\%) &= (\rho_{\text{onelayer}})^{0.5} & \text{if } \rho_{\text{onelayer}} \geq 1.0 \end{aligned} \quad (7)$$

Beam-to-column connections that have an eccentricity between beam and column centerlines are observed to have a reduced capacity when compared to concentric ones. In the generated experimental database; it is seen that maximum shear strength of eccentric connections are about 10 – 15% lower than that of concentric ones. To account for the effect of eccentricity, some geometric properties are investigated and  $e/b_c$  ratio is considered to be the most critical parameter. This parameter is included to the shear strength equation such that as eccentricity increases the strength

decreases. Since the relationship between eccentricity and shear strength is not linear, the square root of the variable is then taken and Eq. (8) is used to define the parameter that accounts for the effect of eccentricity.

$$\text{Eccentricity Effect (EE)} = \sqrt{\frac{1}{1 + e/b_c}} \quad (8)$$

Axial load applied to the column is also considered in the prediction of the joint shear capacity. Axial load provides confinement and a stiffness increase in the joint region, if it is not high enough to prematurely cause crushing. The parameter given in Eq. (9) increases correlation and decreases error while taking into account the effect of axial load. It should be noted that the gross area of the column is used within the parameter because the load is applied before crushing occurs.

$$\text{Axial Load Effect (NE)} = 1 + \frac{N}{A_g \cdot f_c} \quad (9)$$

Because the column dimension in the loading direction, the column depth, is one of the most influential geometric parameters for the performance of beam-to-column connections in moment resisting frame structures subjected to seismic loading, its effect on the proposed equation of joint shear strength was investigated. The ratio of the column width to column depth is known to influence the shear resistance of the connection region (Rafaelle and Wight 1995). Therefore, a parameter, column index (*CI*), is developed and given in Eq. (10). The factor is limited to 1.0 to be used as a penalty factor when the column is loaded along its weak axis.

$$\text{Column Index (CI)} = \begin{cases} \sqrt{\frac{b_c}{h_c}} & \text{when } \frac{b_c}{h_c} < 1.0 \\ 1.0 & \text{when } \frac{b_c}{h_c} \geq 1.0 \end{cases} \quad (10)$$

Slab is another effective means of confinement for the connection region. Some prior studies showed that presence of slab in the floor system provides extra shear strength for the joint region (Burak 2005, Lafave and Wight 1999, Kitayama *et al.* 1991). In order to take the presence of slab into account the effective beam width and the reinforcement placed in the flange can be considered. Therefore, nominal moment strengths ( $M_n$ ) for the beams with T-shaped cross sections are calculated and divided to that of the rectangular sections having same depth and web width. The resulting parameter defines the contribution of the slab. This parameter, slab index (*SI*), is formulized as below

$$SI = \frac{M_n(\text{Flanged Section})}{M_n(\text{Rectangular Section})}; \quad \text{when slab is present}$$

$$SI = 1; \quad \text{when slab is not present} \quad (11)$$

Finally, the effect of wide beams was considered, because as the beams get wider and shallower, the confinement provided to the connection region and therefore, the shear strength of the joint decreases (Burak and Wight 2008). If the depth of the wide beam is less than  $\frac{3}{4}$  of the depth of the adjoining beams as defined in ACI 352-02 (2002), the joint confinement is significantly reduced. The geometric properties of the wide beam are taken into account by multiplying the ratio of beam

depth to beam width, which gives the aspect ratio of the beam section, with the ratio of effective joint width to beam width that indicates the confined region of the joint. The resulting parameter that defines the wide beam effect proposed in the model is shown in Eq. (12):

$$WB = 1 - \frac{h_b}{b_b} \cdot \frac{b_j}{b_b}; \quad \text{when wide beams are present} \\ \text{in the loading direction}$$

Wide Beam Effect (WB) = (12)

$$WB = 1; \quad \text{when wide beams are not present} \\ \text{in the loading direction}$$

The resulting formula for joint shear strength prediction is given in Eq. (13), first in terms of indices, then in terms of individual parameters. Table 3 shows the main properties of the specimens including geometric properties such as column width ( $b_c$ ), column depth ( $h_c$ ), beam width ( $b_b$ ) and beam depth ( $h_b$ ). Material strengths,  $f_c$  and  $f_y$  represent the concrete compressive strength and yield strength of the transverse reinforcement in the joint core respectively. The amount of axial load applied to the column ( $N$ ) and the eccentricity between the centerlines of the column and beam ( $e$ ) are also provided in this table. In this table, the effective joint width values computed by Eq. (3) for connections with normal beams, Eq. (4) for connections with wide beams and Eq. (2) following ACI 352R-02 (2002) recommendations are given. In joint shear strength computations, the effective joint width is selected as the ACI 352R-02 definition for connections with normal beams and Eq. (4) values for connections with wide beams.

$$v_j(\text{MPa}) = JT \cdot (f_c \cdot f_y)^{1/6} \cdot \rho_{joint} \cdot EE \cdot CI \cdot NE \cdot WB \cdot SI$$

$$v_j(\text{MPa}) = JT \cdot (f_c \cdot f_y)^{1/6} \cdot \rho_{joint} \cdot \sqrt{\frac{1}{1 + e/b_c}} \cdot \sqrt{\frac{b_c}{h_c}} \cdot \left(1 + \frac{N}{A_g \cdot f_c}\right) \cdot \left(1 - \frac{h_b}{b_b} \cdot \frac{b_j}{b_b}\right) \cdot SI \quad (13)$$

Table 3 Database of beam-to-column connections

Research Team	Specimen	Joint Type, JT	$f_c$ (MPa)	$f_y$ (MPa)	$b_c$ (mm)	$h_c$ (mm)	$b_b$ (mm)	$h_b$ (mm)	$N$ (kN)	$e$ (mm)	$\rho_{core}$ (%) Eq. 1	$\rho_{gross}$ (%) Eq. 1	$\rho_{onelay}$ (%) Eq. 1	$b_j$ (Eq. 3&4) (mm)	$b_j$ (Eq. ACI 352) (mm)	
Burak & Wight (2005, 2008)	1-S	D	1.25	29.0	441	356	203	381	196	76	1.437	0.952	1.251	280	256	
	2-S	D	1.25	39.0	441	534	356	254	457	289	140	0.794	0.508	0.815	394	307
	3-S	D	1.25	29.0	441	534	356	254	457	234	140	0.794	0.508	0.815	394	307
	2-N	A	1	39.0	441	356	534	305	457	231	0	1.261	0.820	1.314	331	439
	3-N	A	1	29.0	441	356	534	762	305	169	0	1.989	1.228	1.314	559	458
Chen & Chen (1999)	JC	A	1	19.9	399	500	500	300	500	0	0	0.955	0.699	1.141	400	425
	JE	A	1	19.9	399	500	500	300	500	0	100	0.955	0.699	1.141	400	375
Durrani & Wight (1985)	X1	C	1.25	34.3	352	362	362	279	419	245	0	0.753	0.384	0.847	321	321
	X2	C	1.25	33.6	352	362	362	279	419	245	0	1.113	0.576	1.270	321	321
	X3	C	1.25	31.0	352	362	362	279	419	214	0	0.753	0.384	0.847	321	321

Table 3. continued

Research Team	Specimen	Joint Type, $JT$	$f_c$ (MPa)	$f_y$ (MPa)	$b_c$ (mm)	$h_c$ (mm)	$b_b$ (mm)	$h_b$ (mm)	$N$ (kN)	$e$ (mm)	$\rho_{core}$ (%) Eq. 1	$\rho_{gross}$ (%) Eq. 1	$\rho_{nolayer}$ (%) Eq. 1	$b_j$ (Eq. 3&4) (mm)	$b_j$ (Eq. ACI 352) (mm)
Ehsani & Alameddine (1991)	LL8	A 1	55.1	446	356	356	311	508	294	0	1.302	0.643	1.217	333	333
	LH8	A 1	55.1	446	356	356	311	508	294	0	1.952	0.964	2.130	333	333
	HL8	A 1	55.1	446	356	356	311	508	507	0	1.296	0.643	1.278	333	333
	HH8	A 1	55.1	446	356	356	311	508	507	0	1.945	0.964	2.130	333	333
	LL11	A 1	75.8	446	356	356	311	508	285	0	1.302	0.643	1.278	333	333
	LH11	A 1	75.8	446	356	356	311	508	276	0	1.952	0.964	2.130	333	333
	HL11	A 1	75.8	446	356	356	311	508	587	0	1.296	0.643	1.278	333	333
	HH11	A 1	75.8	446	356	356	311	508	605	0	1.945	0.964	2.130	333	333
	LL14	A 1	96.5	446	356	356	311	508	236	0	1.302	0.643	1.278	333	333
	LH14	A 1	96.5	446	356	356	311	508	222	0	1.952	0.964	2.130	333	333
HH14	A 1	96.5	446	356	356	311	508	476	0	1.945	0.964	2.130	333	333	
Ehsani & Wight (1985)	1B	A 1	33.6	437	300	300	259	480	178	0	0.687	0.424	1.320	279	279
	2B	A 1	34.9	437	300	300	259	439	222	0	0.759	0.463	1.489	279	279
	3B	A 1	40.9	437	300	300	259	480	222	0	1.030	0.636	1.759	279	279
	4B	A 1	44.6	437	300	300	259	439	222	0	1.114	0.694	1.935	279	279
	5B	A 1	24.3	437	340	340	300	480	356	0	0.594	0.384	1.167	320	320
	6B	A 1	39.8	437	340	340	300	480	303	0	0.594	0.384	1.090	320	320
Fujii & Morita (1991)	A1	C 1.25	40.2	297	220	220	160	250	147	0	0.400	0.251	0.592	190	190
	A2	C 1.25	40.2	297	220	220	160	250	147	0	0.400	0.251	0.592	190	190
	A3	C 1.25	40.2	297	220	220	160	250	441	0	0.400	0.251	0.592	190	190
	A4	C 1.25	40.2	297	220	220	160	250	441	0	1.066	0.669	1.690	190	190
	B1	A 1	30.0	297	220	220	160	250	98	0	0.400	0.251	0.592	190	190
	B2	A 1	30.0	297	220	220	160	250	98	0	0.400	0.251	0.592	190	190
	B3	A 1	30.0	297	220	220	160	250	343	0	0.400	0.251	0.592	190	190
	B4	A 1	30.0	297	220	220	160	250	343	0	1.066	0.669	1.690	190	190
Gentry & Wight (1994)	1	B 1.25	27.6	441	356	356	864	305	89	0	0.541	0.331	0.676	610	483
	2	B 1.25	27.6	441	356	356	762	305	89	0	0.541	0.331	0.676	559	457
	3	B 1.25	27.6	441	356	356	864	305	89	0	0.541	0.331	0.676	610	483
	4	B 1.25	27.6	441	356	356	864	305	89	0	0.541	0.331	0.676	610	483
Guimaraes, Kreger & Jirsa (1992)	J2	E 1.67	27.6	549	508	508	406	508	0	0	0.593	0.364	0.841	457	457
	J4	E 1.67	31.6	549	508	508	406	508	0	0	0.791	0.486	0.841	457	457
	J5	E 1.67	77.9	511	508	508	406	508	0	0	1.753	1.077	2.484	457	457
	J6	E 1.67	92.1	511	508	508	406	508	0	0	1.753	1.077	2.484	457	457

Table 3 continued

Research Team	Specimen	Joint Type, $JT$	$f_c$ (MPa)	$f_y$ (MPa)	$b_c$ (mm)	$h_c$ (mm)	$b_b$ (mm)	$h_b$ (mm)	$N$ (kN)	$e$ (mm)	$\rho_{core}$ (%) Eq. 1	$\rho_{gross}$ (%) Eq. 1	$\rho_{onelayer}$ (%) Eq. 1	$b_j$ (Eq. 3&4) (mm)	$b_j$ (Eq. ACI 352) (mm)
Kaku & Asakusa (1991)	Specimen 1	A 1	31.1	250	220	220	160	220	258	0	0.496	0.433	0.503	190	190
	Specimen 2	A 1	41.7	250	220	220	160	220	199	0	0.496	0.433	0.503	190	190
	Specimen 3	A 1	41.7	250	220	220	160	220	0	0	0.496	0.433	0.503	190	190
	Specimen 4	A 1	44.7	281	220	220	160	220	360	0	0.129	0.107	0.131	190	190
	Specimen 5	A 1	36.7	281	220	220	160	220	160	0	0.129	0.107	0.131	190	190
	Specimen 6	A 1	40.4	281	220	220	160	220	0	0	0.129	0.107	0.131	190	190
	Specimen 7	A 1	32.2	250	220	220	160	220	194	0	0.496	0.433	0.503	190	190
	Specimen 8	A 1	41.2	250	220	220	160	220	160	0	0.496	0.433	0.503	190	190
	Specimen 9	A 1	40.6	250	220	220	160	220	0	0	0.496	0.433	0.503	190	190
	Specimen 10	A 1	44.4	281	220	220	160	220	360	0	0.129	0.107	0.131	190	190
	Specimen 11	A 1	41.9	281	220	220	160	220	160	0	0.129	0.107	0.131	190	190
	Specimen 12	A 1	35.1	281	220	220	160	220	0	0	0.129	0.107	0.131	190	190
	Specimen 13	A 1	46.4	250	220	220	160	220	-100	0	0.496	0.433	0.503	190	190
	Specimen 14	A 1	41.0	281	220	220	160	220	160	0	0.128	0.108	0.129	190	190
	Specimen 15	A 1	39.7	281	220	220	160	220	160	0	0.128	0.108	0.129	190	190
	Specimen 16	A 1	37.4	250	220	220	160	220	0	0	0.489	0.440	0.496	190	190
	Specimen 17	A 1	39.7	250	220	220	160	220	0	0	0.496	0.433	0.503	190	190
	Specimen 18	A 1	40.7	250	220	220	160	220	0	0	0.491	0.438	0.498	190	190
Kitayama, Otani & Aoyama (1991)	A1	C 1.25	30.6	326	300	300	200	300	177	0	0.368	0.239	0.708	250	250
	A2	E 1.67	30.6	326	300	300	200	300	177	0	0.368	0.239	0.708	250	250
	A3	E 1.67	30.6	326	300	300	200	300	177	0	0.368	0.239	0.708	250	250
	A4	C 1.25	30.6	326	300	300	200	300	177	0	0.368	0.239	0.708	250	250
LaFave & Wight (1999)	EWB 1	B 1.25	28.9	482	356	356	864	305	0	0	0.811	0.497	0.772	610	483
	EWB 2	B 1.25	30.3	482	356	356	864	305	0	0	0.811	0.497	0.772	610	483
	EWB 3	B 1.25	34.5	482	305	508	940	305	0	0	1.298	0.811	1.081	622	464
	ENB 1	B 1.25	24.8	482	305	508	305	559	0	0	0.811	0.553	1.081	305	432
Lee & Ko (2007)	S0	A 1	32.6	471	400	600	300	450	700	0	0.326	0.216	0.423	350	350
	S50	A 1	34.2	471	400	600	300	450	700	50	0.326	0.216	0.423	350	350
	W0	A 1	28.9	471	600	400	300	450	700	0	0.872	0.578	1.134	450	450
	W75	A 1	30.4	471	600	400	300	450	700	75	0.872	0.578	1.134	450	450
	W150	A 1	29.1	471	600	400	300	450	700	150	0.872	0.578	1.134	450	450

Table 3 continued

Research Team	Specimen	Joint Type, $JT$	$f_c$ (MPa)	$f_y$ (MPa)	$b_c$ (mm)	$h_c$ (mm)	$b_b$ (mm)	$h_b$ (mm)	$N$ (kN)	$e$ (mm)	$\rho_{core}$ (%) Eq. 1	$\rho_{gross}$ (%) Eq. 1	$\rho_{onelayer}$ (%) Eq. 1	$b_j$ (Eq. 3&4) (mm)	$b_j$ (Eq. 352) (mm)	
Oka & Shiohara (2001)	J-7	C	1.25	79.2	857	300	300	240	300	834	0	0.718	0.368	0.689	270	270
	J-10	C	1.25	39.2	598	300	300	240	300	834	0	0.718	0.368	0.689	270	270
Quintero-Febres & Wight (2001)	IWB1	E	1.67	27.6	503	356	356	889	305	0	0	1.070	0.655	1.097	622	489
	IWB2	E	1.67	27.6	503	356	356	660	305	0	0	1.070	0.655	1.097	508	432
	IWB3	E	1.67	27.6	503	330	508	838	305	0	0	1.180	0.749	0.908	584	457
Raffaella & Wight (2001)	1	C	1.25	28.6	441	356	356	254	381	89	51	0.624	0.397	0.772	305	307
	2	C	1.25	26.8	441	356	356	178	381	89	89	0.624	0.397	0.772	267	231
	3	C	1.25	37.7	441	356	356	191	381	89	83	0.624	0.397	0.772	273	244
	4	C	1.25	19.3	441	356	356	191	559	89	83	0.624	0.451	0.772	273	244
Shin & LaFave (2004, 2004)	SL 1	D	1.25	29.9	468	457	330	279	406	0	89	0.429	0.282	0.615	368	329
	SL 2	D	1.25	36.1	468	457	330	178	406	0	140	0.429	0.282	0.615	318	227
	SL 3	D	1.25	47.4	551	457	330	279	406	0	0	0.429	0.282	0.615	368	362
	SL 4	D	1.25	31.1	579	279	368	279	406	0	0	0.765	0.472	1.099	279	279
Teng & Zhou (2008)	S1	C	1.25	33.0	440	400	300	200	400	441	0	0.593	0.339	0.885	300	275
	S2	C	1.25	34.0	440	400	300	200	400	441	50	0.593	0.339	0.885	300	275
	S3	C	1.25	35.0	440	400	300	200	400	441	100	0.593	0.339	0.885	300	245
	S5	C	1.25	39.0	440	400	200	200	400	343	50	0.580	0.287	1.287	300	250
	S6	C	1.25	38.0	440	400	200	200	400	343	100	0.580	0.287	1.287	300	230
	Minimum		19.3	250	220	200	160	220	-100	0	0.1	0.1	0.1	190	215	
	Maximum		96.5	857	600	600	939.8	558.8	834	150	2	1.2	2.5	622.3	533.4	
	Average		40.3	404.1	337.2	330.6	308.5	366.1	221.1	17.0	0.8	0.5	1.0	322.8	330.8	
	Standard Deviation		17.3	103.6	100.1	99.7	207.5	110.7	217.1	38.6	0.5	0.3	0.6	126.8	102.3	

### 5. Discussion of results

Predicted joint shear strength values obtained from Eq. (13) and their comparison with the experimental ones are presented in Table 4. In order to make an evaluation, joint shear strength values computed by following the ACI 352R-02 recommendations (Eq. (14)) are also given in the table. The error between the predicted and experimental values, predicted and code-recommended values and finally code-recommended and experimental values are also provided. The error formula, which is given by Eq. (15), can be utilized to test the accuracy of the equation. The average error between predicted and experimental values of joint shear strength is -4.2% whereas the absolute average error is 14.4%. This error can be regarded as acceptable, because bar slip was not directly

Table 4 Joint shear strength prediction

Research Team	Specimen	Joint Transverse Reinforcement	Failure Mode	$v_{j-experimental}$ (Mpa)	$v_{j-predicted}$ (Mpa), Eq. (13)	$v_{j-ACI}$ (Mpa), Eq. (14)	% error between $v_{j-predicted}$ and $v_{j-experimental}$ , Eq. (15)	% error between $v_{j-ACI}$ and $v_{j-experimental}$ , Eq. (16)	% error between $v_{j-predicted}$ and $v_{j-ACI}$ , Eq. (17)
Burak & Wight (2005, 2008)	1-S	C	BJ	8.51	7.17	6.70	-15.72	-21.24	7.01
	2-S	C	BJ	7.88	6.70	7.78	-14.97	-1.29	-13.86
	3-S	C	BJ	7.56	6.52	6.70	-13.75	-11.28	-2.78
	2-N	C	BJ	4.88	5.45	7.78	11.66	59.17	-29.85
	3-N	C	BJ	3.38	3.84	6.70	13.30	98.08	-42.80
Chen & Chen (1999)	JC	C	BJ	3.63	4.77	4.45	31.48	22.48	7.35
	JE	C	BJ	3.77	4.36	4.44	15.61	17.91	-1.95
Durrani & Wight (1985)	X1	NC	BJ	6.17	6.31	7.29	2.32	18.19	-13.43
	X2	NC	BJ	6.83	7.10	7.22	3.95	5.71	-1.67
	X3	NC	BJ	6.09	6.20	6.93	1.71	13.77	-10.60
Ehsani & Alameddine (1991)	LL8	NC	BJ	7.26	6.20	7.39	-14.57	1.90	-16.16
	LH8	NC	BJ	7.07	8.20	7.39	16.01	4.60	10.91
	HL8	NC	J	8.32	6.54	7.39	-21.42	-11.15	-11.56
	HH8	NC	BJ	8.31	8.44	7.39	1.53	-11.07	14.17
	LL11	NC	J	6.49	6.62	8.67	2.03	33.65	-23.66
	LH11	NC	BJ	7.88	8.54	8.67	8.35	10.04	-1.54
	HL11	NC	J	8.16	6.82	8.67	-16.41	6.25	-21.32
	HH11	NC	BJ	8.61	8.82	8.67	2.45	0.69	1.75
	LL14	NC	BJ	7.40	6.82	9.78	-7.86	32.13	-30.27
	LH14	NC	BJ	7.51	8.80	9.78	17.10	30.22	-10.07
HH14	NC	BJ	8.71	8.98	9.78	3.07	12.32	-8.24	
Ehsani & Wight (1985)	1B	C	J	7.33	6.02	5.77	-17.89	-21.28	4.31
	2B	C	J	7.48	6.51	5.89	-13.00	-21.28	10.52
	3B	C	BJ	7.29	7.19	6.37	-1.37	-12.67	12.94
	4B	C	BJ	7.44	7.62	6.65	2.41	-10.58	14.52
	5B	C	J	6.62	5.70	4.91	-13.86	-25.82	16.13
	6B	C	J	4.90	5.66	6.28	15.56	28.12	-9.81
Fujii & Morita (1991)	A1	NC	J	9.86	6.43	6.31	-34.79	-35.93	1.78
	A2	NC	J	9.08	6.43	6.31	-29.23	-30.47	1.78
	A3	NC	J	9.86	7.33	6.31	-25.63	-35.93	16.08
	A4	C	J	10.07	9.53	6.31	-5.35	-37.28	50.91
	B1	NC	J	5.89	4.86	6.82	-17.48	15.76	-28.72
	B2	NC	BJ	5.12	4.86	6.82	-4.99	33.28	-28.72
	B3	NC	J	6.52	5.63	6.82	-13.73	4.52	-17.46
	B4	C	J	6.88	7.32	6.82	6.41	-0.83	7.31

Table 4 continued

Research Team	Specimen	Joint Transverse Reinforcement	Failure Mode	$v_{j-experimental}$ (Mpa)	$v_{j-predicted}$ (Mpa), Eq. (13)	$v_{j-ACI}$ (Mpa), Eq. (14)	% error between $v_{j-predicted}$ and $v_{j-experimental}$ , Eq. (15)	% error between $v_{j-ACI}$ and $v_{j-experimental}$ , Eq. (16)	% error between $v_{j-predicted}$ and $v_{j-ACI}$ , Eq. (17)
Gentry & Wight (1994)	1	C	J	4.36	4.93	6.54	13.24	50.00	-24.51
	2	C	B	4.49	4.67	6.54	3.98	45.48	-28.53
	3	C	BJ	4.95	4.93	6.54	-0.23	32.16	-24.51
	4	C	B	5.60	4.93	6.54	-11.92	16.67	-24.51
Guimaraes, Kreger & Jirsa (1992)	J2	C	BJ	10.58	9.24	8.73	-12.72	-17.54	5.85
	J4	C	BJ	9.73	9.53	9.34	-2.02	-4.03	2.10
	J5	C	BJ	18.19	17.15	14.65	-5.72	-19.46	17.06
	J6	C	BJ	16.58	17.54	15.93	5.80	-3.95	10.16
Kaku & Asakusa (1991)	Specimen 1	C	B	6.20	5.21	5.55	-15.91	-10.41	-6.13
	Specimen 2	C	B	6.20	5.13	6.43	-17.18	3.74	-20.17
	Specimen 3	C	BJ	5.30	4.67	6.43	-11.81	21.35	-27.33
	Specimen 4	NC	BJ	6.00	5.62	6.66	-6.27	10.98	-15.55
	Specimen 5	NC	BJ	5.20	5.09	6.03	-2.20	16.04	-15.71
	Specimen 6	NC	BJ	5.10	4.74	6.33	-7.04	24.13	-25.11
	Specimen 7	C	B	6.30	5.03	5.65	-20.09	-10.29	-10.93
	Specimen 8	C	B	6.10	5.04	6.39	-17.40	4.80	-21.18
	Specimen 9	C	BJ	6.00	4.65	6.35	-22.45	5.77	-26.68
	Specimen 10	NC	B	6.05	5.62	6.64	-7.06	9.70	-15.28
	Specimen 11	NC	BJ	6.00	5.15	6.45	-14.23	7.45	-20.18
	Specimen 12	NC	BJ	5.00	4.63	5.90	-7.38	18.02	-21.52
	Specimen 13	NC	BJ	5.30	4.55	6.78	-14.23	28.01	-32.99
	Specimen 14	NC	BJ	5.90	5.14	6.38	-12.96	8.09	-19.47
	Specimen 15	NC	BJ	6.00	5.12	6.28	-14.66	4.59	-18.40
	Specimen 16	C	B	6.10	4.59	6.09	-24.76	-0.15	-24.65
	Specimen 17	C	CJ	4.40	4.64	6.28	5.36	42.63	-26.13
	Specimen 18	C	C	3.00	4.66	6.35	55.17	111.80	-26.74
Kitayama, Otani & Aoyama (1991)	A1	NC	J	9.18	6.17	6.89	-32.79	-24.99	-10.40
	A2	NC	B	11.02	8.23	9.18	-25.32	-16.65	-10.40
	A3	NC	B	12.24	8.96	6.89	-26.79	-43.74	30.14
	A4	NC	J	9.49	6.72	9.18	-29.15	-3.21	-26.80

Table 4 continued

Research Team	Specimen	Joint Transverse Reinforcement	Failure Mode	$v_{j-experimental}$ (Mpa)	$v_{j-predicted}$ (Mpa), Eq. (13)	$v_{j-ACI}$ (Mpa), Eq. (14)	% error between $v_{j-predicted}$ and $v_{j-experimental}$ , Eq. (15)	% error between $v_{j-ACI}$ and $v_{j-experimental}$ , Eq. (16)	% error between $v_{j-predicted}$ and $v_{j-ACI}$ , Eq. (17)
LaFave & Wight (1999)	EWB 1	C	B	5.34	5.16	6.70	-3.50	25.33	-23.00
	EWB 2	C	B	4.94	5.16	6.85	4.60	38.85	-24.67
	EWB 3	C	B	4.75	4.49	7.31	-5.50	53.92	-38.61
	ENB 1	C	B	2.96	5.11	6.20	72.65	109.49	-17.58
Lee & Ko (2007)	S0	NC	B	3.94	4.44	5.69	12.49	44.23	-22.01
	S50	NC	B	3.76	4.20	5.82	11.76	55.03	-27.91
	W0	C	BJ	4.84	5.73	5.35	18.26	10.54	6.98
	W75	C	BJ	4.88	5.42	5.49	11.22	12.65	-1.27
	W150	C	BJ	4.93	5.13	5.37	3.97	8.97	-4.59
Oka & Shiohara (2001)	J-7	NC	BJ	10.49	8.92	11.08	-15.02	5.58	-19.51
	J-10	NC	J	12.35	8.27	7.79	-33.03	-36.86	6.07
Quintero-Febrés & Wight (2001)	IWB1	C	NF	5.39	7.11	8.71	31.96	61.64	-18.36
	IWB2	C	NF	6.82	6.49	8.71	-4.95	27.72	-25.58
	IWB3	C	NF	5.35	5.50	8.71	2.75	62.77	-36.88
Raffaella & Wight (1995)	1	C	BJ	6.00	5.78	6.66	-3.74	10.88	-13.18
	2	C	BJ	5.12	5.55	6.45	8.37	25.96	-13.97
	3	NC	BJ	5.42	5.79	7.64	6.97	41.09	-24.18
	4	C	BJ	4.76	5.27	5.47	10.89	14.99	-3.56
Shin & LaFave (2004, 2004)	SL 1	C	BJ	5.94	6.06	6.81	2.13	14.64	-10.92
	SL 2	NC	BJ	8.65	6.40	7.48	-26.01	-13.54	-14.43
	SL 3	NC	B	5.58	7.25	8.57	29.79	53.54	-15.47
	SL 4	C	BJ	7.56	6.56	6.95	-13.22	-8.16	-5.51
Teng & Zhou (2008)	S1	NC	BJ	8.60	6.86	7.15	-20.21	-16.84	-4.06
	S2	NC	BJ	8.60	6.48	7.26	-24.62	-15.59	-10.71
	S3	NC	BJ	8.30	6.16	7.37	-25.76	-11.26	-16.34
	S5	NC	BJ	7.50	7.54	7.78	0.49	3.67	-3.07
	S6	NC	BJ	7.30	7.14	7.67	-2.23	5.13	-7.00

C: Specimens having code compliant transverse reinforcement, NC: Specimens having lower transverse reinforcement than the amount required by the code (2002)

J: Joint Failure (Yielding of transverse reinforcement or crushing of concrete strut), B: Yielding of Beam Reinforcement, BJ: Beam Bar Yielding followed by Joint Failure, C: Column Failure, CJ: Column Bar Yielding followed by Joint Failure, NF: No Failure

taken into account and when joint shear strength was computed from the strain gage data, which might sometimes be affected by the noise in the environment, the error increases.

$$v_{j-ACI}(\text{MPa}) = 0.083 \cdot \gamma \cdot \sqrt{f'_c} \tag{14}$$

$$\% \text{ error between predicted and experimental } v_j : \frac{(v_{j-predicted}) - (v_{j-exp.})}{(v_{j-exp.})} \tag{15}$$

$$\% \text{ error between predicted and code-recommended } v_j : \frac{(v_{j-predicted}) - (v_{j-ACI})}{(v_{j-ACI})} \tag{16}$$

$$\% \text{ error between code-recommended and experimental } v_j : \frac{(v_{j-ACI}) - (v_{j-exp.})}{(v_{j-exp.})} \tag{17}$$

where,  $v_{j-exp.}$  is the experimental joint shear strength

$v_{j-predicted}$  is the joint shear strength computed by Eq. 13

$v_{j-ACI}$  is the joint shear strength computed by Eq. 14, where  $\gamma$  is the shear strength factor reflecting confinement of joint by lateral members as defined in ACI-ASCE Committee 352 Recommendations (2002).

In order to compare the predicted values with the experimental ones, linear correlation coefficient defined in Eq. (5) is utilized. In the resulting model, a correlation of 88% is obtained between the predicted and experimental values of joint shear strength. As compared to correlations of individual parameters with the experimental joint shear strength, the resulting formula, which is the combination of these parameters, gives a much higher correlation. This proves the validation of the method utilized in this study. Experimental versus predicted values of joint shear strength for all specimens are shown in Fig. 5. For lower joint shear strength levels, the predicted values are closer to experimental ones. However, as the strength values get larger, the error increases. The overall

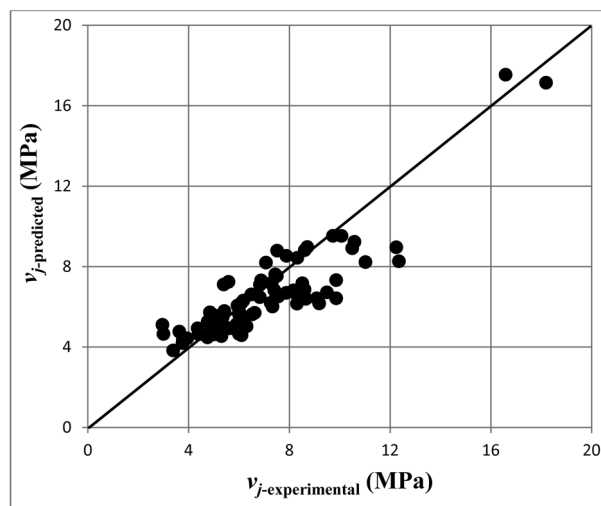


Fig. 5 Predicted versus experimental joint shear strength

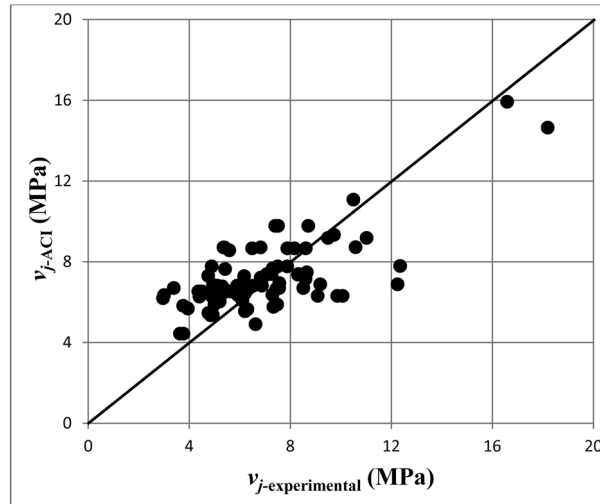


Fig. 6 ACI 352-02 (2002) recommended versus experimental joint shear strength

trend of the graphical comparison shows a slight underestimation of strength which is conservative. In Fig. 6, the comparison of the joint shear strength values computed by ACI equation with the experimental ones are presented. As it can be observed from this figure, the proposed formula gives more conservative results with less scatter when compared to the equation recommended by ACI 352 R-02.

It is observed from the prediction results that the proposed model yields more accurate predictions for interior connections when compared to exterior ones. This may be due to higher uncertainty involved in exterior connections resulting from the confinement effect. On the other hand, presence of wide beams also affects the predictions negatively. Although a parameter,  $WB$ , is defined in order to account for the presence of wide beams and reduce the error, it can still be observed that connections without wide beams have closer predictions. One of the most important advantages of this model is that the eccentricity is taken into account. The predictions for the eccentric connections are significantly close to the experimental values.

## 6. Conclusions

The main objective of this study is to develop an equation to accurately predict the joint shear strength of reinforced concrete beam-to-column connections subjected to earthquake loading. First, an experimental database of reinforced concrete connections is generated which includes geometric characteristics and material properties of the specimens and the test results under cyclic loading. Then, the statistical correlation of key parameters that influences the seismic behavior of beam-to-column connections with the experimental joint shear strength is investigated individually. The key parameters are determined and incorporated into the joint shear prediction equation. Final parameters are defined in terms of ratios and powers of some of the key individual parameters to accurately represent their effect on the capacity and obtain the minimum average error and the highest correlation with the experimental values. While carrying out these steps, the guidelines

given in ACI Committee 318 (2008), Building Code Requirements for Structural Concrete and ACI-ASCE Committee 352 (2002), Recommendations for Design of Beam-Column Connections in Monolithic Reinforced Concrete Structures are followed. Based on the results of this analytical investigation, the following conclusions are drawn

1. Statistical correlations indicated that the most influential factors on shear strength of reinforced concrete beam-to-column connections are compressive strength of concrete, volumetric joint transverse reinforcement ratio and effective joint width. Presence of eccentricity between the longitudinal beam and the column centerlines, axial load applied to the column and presence of wide beams and slab also have significant effect on the behavior of connections subjected to cyclic loading.
2. A statistical combination of the key parameters is used to predict the joint shear strength and the average error turned out to be -4.2% whereas the absolute average error is 14.4%. The correlation between experimental and predicted joint shear strengths is 88%.
3. Although a low number of the shear strength predictions are higher than the experimental values, the proposed formula is generally conservative. Furthermore, since the guidelines of ACI 352R-02 (2002) are followed, it is suitable for design applications.
4. The predicted formula gives closer results to the experimental data for well-detailed connection regions that are designed following the ACI 318-08 (2008) and ACI 352-02 (2002) design codes.
5. The proposed formula for joint shear strength prediction gives more conservative results with less scatter when compared to the equation recommended by ACI 352 R-02.
6. The significance of concrete compressive strength and volumetric joint transverse reinforcement ratio on the joint shear response is also verified by this analytical study.

## References

- ACI Committee 318 (2008), "Building code requirements for structural concrete", ACI 318-08, *American Concrete Institute*, Farmington Hills, Michigan.
- ACI-ASCE Committee 352 (2002), "Recommendations for Design of Beam-Column Connections in Monolithic Reinforced Concrete Structures", *ACI 352R-02, American Concrete Institute*, Farmington Hills, Michigan.
- Burak, B. (2005), "Seismic behavior of eccentric reinforced concrete beam-column-slab connections", Ph.D. Thesis, The University of Michigan, Ann Arbor.
- Burak, B. and Wight, J.K. (2008), "Experimental investigation on seismic behavior of eccentric reinforced concrete beam-column-slab connections", *ACI Struct. J.*, **105**(S16), 154-162.
- Chen, C.C. and Chen, G. (1999), "Cyclic behavior of reinforced concrete eccentric beam-column corner joints connecting spread-ended beams", Technical Paper, *ACI Struct. J.*, **96**(S50), 443-450.
- Durrani, A. J. and Wight, J. K. (1985), "Behavior of interior beam-to-column connections under earthquake-type loading", *ACI Struct. J.*, **82**(30), 343-349.
- Ehsani, M.R. and Alameddine, F. (1991), "Design recommendations for type 2 high-strength reinforced concrete connections", Technical Paper, *ACI Struct. J.*, **88**(S30), 277-290.
- Ehsani, M.R. and Wight J.K. (1985), "Exterior reinforced concrete beam-to-column connections subjected to earthquake-type loading", Technical Paper, *ACI Struct. J.*, **82**(43), 492-499.
- Fujii, S. and Morita, S. (1991). "Comparison between interior and exterior RC beam-column joint behavior", *ACI SP-123 Design of Beam-Column Joints for Seismic Resistance, American Concrete Institute*, Michigan, 145-165.
- Gentry, T.R. and Wight, J.K. (1994), "Wide beam-column connections under earthquake-type loading", *Earthq. Spectra*, **10**(4), 675-702.
- Guimaraes, G.N., Kreger, M.E. and Jirsa, J.O. (1992), "Evaluation of joint-shear provisions for interior beam-

- column-slab connections using high-strength materials”, Technical Paper, *ACI Struct. J.*, **89**(S10), 89-98.
- Kaku, T. and Asakusa, H. (1991). *Ductility Estimation of Exterior Beam-Column Subassemblages in Reinforced Concrete Frames, Design of Beam-Column Joints for Seismic Resistance*, ACI SP-123, 167-185.
- Kim, J. and LaFave, J. (2008), “Probabilistic joint shear strength models for design of RC beam-column connections”, *ACI Struct. J.*, **105**(S71), 770-780.
- Kitayama, K., Otani, S. and Aoyama, H. (1991), “Development of design criteria for RC interior beam-column joints”, *ACI SP-123 Design of Beam-Column Joints for Seismic Resistance*, American Concrete Institute, Michigan.
- LaFave, J.M. and Wight, J.K. (1999), “Reinforced concrete exterior wide beam-column-slab connections subjected to lateral earthquake loading”, *ACI Struct. J.*, **96**(S64), 577-586.
- LaFave, J.M., Bonacci, J.F., Burak, B. and Shin, M. (2005), “Eccentric beam-column connections-performance and design of joints subjected to seismic lateral load reversals”, *Concrete Int.*, **27**(9), 58-62.
- Lee, H.J. and Ko, J. (2007), “Eccentric reinforced concrete beam-column connections subjected to cyclic loading in principal directions”, *ACI Struct. J.*, **104**(S44), 459-467.
- Lowes, N.L. and Altoontash, A. (2003), “Modeling of reinforced-concrete beam-column joints subjected to cyclic loading”, *J. Struct. Eng.*, SACE, **129**(12), 1686-1697.
- Mitra, N. and Lowes, N. L. (2007), “Evaluation, calibration, and verification of a reinforced concrete beam-column joint model”, *J. Struct. Eng.*, ASCE, **133**(1), 105-120.
- Quintero-Febres, C.G. and Wight, J.K. (2001), “Experimental study of reinforced concrete interior wide beam-column connections subjected to lateral loading”, *ACI Struct. J.*, **98**(S55), 572-581.
- Rafaelle, S. G. and Wight, J.K. (1995), “Reinforced concrete eccentric beam-column connections subjected to earthquake-type loading”, *ACI Struct. J.*, **92**(S6), 45-55.
- Shin, M. and LaFave, J.M. (2004), “Modeling of cyclic joint shear deformation contributions in RC beam-column connections to overall frame behavior”, *Struct. Eng. Mech.*, **18**(5), 645-669.
- Shin, M. and LaFave, J.M. (2004), “Reinforced concrete edge beam-column-slab connections subjected to earthquake loading”, *Mag. Concrete Res.*, **56**(5), 273-291.
- Shiohara, H. (2001), “New model for shear failure of RC interior beam-column connections”, *J. Struct. Eng.*, ASCE, **127**(2), 152-160.
- Teng, S. and Zhou, H. (2008), “Eccentric reinforced concrete beam-column joints subjected to cyclic loading”, *ACI Struct. J.*, **100**(S15), 139-148.
- Unal, M. (2010), “Analytical modeling of reinforced concrete beam-to-column connections”, M.Sc. Thesis, Middle East Technical University, Ankara, Turkey.